

THE PRODUCTION OF HIGGS BOSON AND HEAVY FERMION PAIR IN ELECTRON-POSITRON COLLISIONS

S.K. ABDULLAYEV^{1,a}, M.Sh. GOJAYEV^{1,b}

^{1,2}*Baku State University, Faculty of Physics, Department of Theoretical Physics,
Azerbaijan. AZ 1148, Baku, Acad. Z. Khalilov, 23*

e-mail: ^a*s_abdullayev@bsu.edu.az*, ^b*m_qocayev@mail.ru*

Taking into account the arbitrary polarizations of the electron-positron pair and longitudinal polarizations of the fermionic pair, the differential cross sections of the Higgs boson and the heavy fermion pair production in electron-positron annihilation are calculated: $e^-e^+ \rightarrow H_{SM} f \bar{f}$, $e^-e^+ \rightarrow H f \bar{f}$, $e^-e^+ \rightarrow h f \bar{f}$ and $e^-e^+ \rightarrow A f \bar{f}$. Characteristic features of the behavior of the cross sections, angular and spin correlations are investigated as a function of the scaling energies and the emission angles of the particles.

Keywords: Standard Model, Higgs boson, fermion pair, helicity, coupling constant, Minimal Supersymmetric Standard model.

PACS: 12.15.-y, 12.60.-i, 13.66.Fg, 14.70. Hp, 14.80.Bn.

DOI: 10.1016/j.physrep.2007.10.005

INTRODUCTION

The Standard Model (SM), based on a gauge theory with a symmetry group $SU(3)_C \times SU(2)_L \times U(1)$, quantitatively describes the physics of strong, electromagnetic, and weak interactions between leptons and quarks [1, 2]. In physics of elementary particles, no experiments have yet been observed, the results of which do not agree with the SM. Recently opened nedostayuschy brick in the building SM. This is a scalar Higgs boson, discoveries by ATLAS and CMS collaborations [3, 4] in the Large Hadron Collider (LHC). The discovery of the Higgs boson has experimentally confirmed the theoretically predicted mechanism of mass generation of fundamental particles – the mechanism of spontaneous Breit-Englert-Higgs symmetry breaking [5].

In the first experiments conducted in the LHC, the main properties of this particle are established: the Higgs boson is a scalar particle with a positive parity, a nonvanishing vacuum value of about 125 GeV, interacting with W^\pm - and Z^0 -bosons with a constant proportional to their masses. With the discovery of Higgs boson, SM entered a new stage in the study of the properties of fundamental interactions of elementary particles. In this connection, interest in various channels for the production and decay of the Higgs boson has greatly increased [6-12].

We note that the collision of high-energy electrons and positrons is an effective method for studying the mechanisms of interaction of elementary particles. This is mainly due to two reasons. First, the interaction of electrons and positrons is described by the electroweak

theory, and therefore the results obtained are well interpreted. Secondly, electrons and positrons do not participate in strong interactions, as a result of which the background conditions of experiments are substantially improved in comparison with the studies carried out with beams of hadrons. At present, electron-positron colliders of high energies are designed to study the physical properties of Higgs bosons: ILC, CLIC, FCC [13, 14], as well as muon colliders [15].

In a recent paper [10], we investigated the production of the Higgs boson and light fermion pair in arbitrarily polarized electron-positron collisions. In this paper we discuss the processes of the joint production of a Higgs boson and a longitudinally polarized heavy fermion pair in arbitrarily polarized electron-positron beams:

$$e^- + e^+ \rightarrow H_{SM} + f + \bar{f}, \quad (1)$$

where $f \bar{f}$ it can be a lepton $\tau^- \tau^+$ -pair or a $b \bar{b}$ -, $t \bar{t}$ -quark pair

1. Calculation of the square of the matrix element

We assume that in a e^-e^+ -collision a heavy fermion pair is produced by an electromagnetic mechanism, and then a scalar Higgs boson H_{SM} is braked by the fermion and antifermion (see Fig. 1, where Feynman diagrams are illustrated, in the diagrams, 4-particle impulses are written in parentheses).

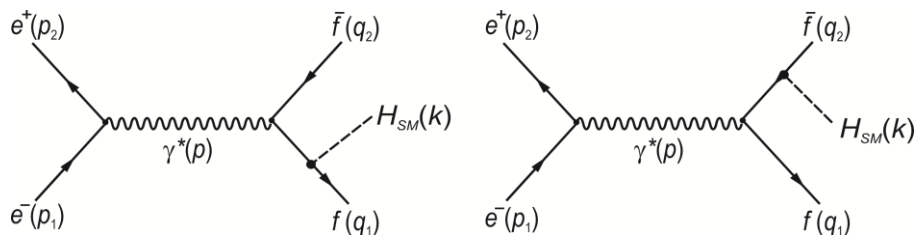


Fig. 1. Feynman diagrams of the process $e^-e^+ \rightarrow H_{SM} f \bar{f}$

Note that this reaction can occur due to a weak mechanism $e^- + e^+ \rightarrow (Z^*) \rightarrow H_{SM} + f + \bar{f}$, however, this mechanism is not considered here.

The following matrix element corresponds to the diagrams given:

$$M_{i \rightarrow f} = \frac{e^2 Q_f}{s} g_{H_{SM} f \bar{f}} \cdot [\bar{v}(p_2) \gamma_\mu u(p_1)] \cdot J_\mu, \quad (2)$$

where

$$J_\mu = \bar{u}_f(q_1) \left[\frac{\hat{q}_1 + \hat{k} + m_f}{(q_1 + k)^2 - m_f^2} \gamma_\mu - \gamma_\mu \frac{\hat{q}_2 + \hat{k} - m_f}{(q_2 + k)^2 - m_f^2} \right] v_f(q_2) \quad (3)$$

is fermionic electromagnetic current, $s = p^2 = (p_1 + p_2)^2$ – the square of the total energy of the electron and positron in the center of mass system, m_f and Q_f are the mass and electric charge of the fermion correspondingly, $g_{H_{SM} f \bar{f}}$ is the constant of the Higgs interaction of the boson with the fermion pair. According to the SM, this constant is proportional to the mass of the fermion

$$g_{H_{SM} f \bar{f}} = \frac{m_f}{\eta} = m_f [\sqrt{2} G_f]^{1/2}.$$

Here $\eta = 246$ GeV is the vacuum value of the Higgs bosonic field, G_F is the Fermi constant of weak interactions.

The square of the matrix element (2) is expressed by the formula

$$|M_{i \rightarrow f}|^2 = \frac{e^4 Q_f^2}{s^2} g_{H_{SM} f \bar{f}}^2 L_{\mu\nu} H_{\mu\nu}. \quad (4)$$

Here $L_{\mu\nu}$ and $H_{\mu\nu}$ are the conserved lepton and fermionic tensors

$$L_{\mu\nu} p_\mu = L_{\mu\nu} p_\nu = H_{\mu\nu} p_\mu = H_{\mu\nu} p_\nu = 0.$$

As a result, in the center-of-mass system, only the spatial components of these tensors contribute to the cross section:

$$L_{\mu\nu} H_{\mu\nu} = L_{mr} H_{mr} \quad (m, r = 1, 2, 3).$$

The tensor L_{mr} can easily be calculated on the basis of the matrix element (2), and in the case of annihilation of an arbitrarily polarized $e^- e^+$ -pair, the structure has the following structure [16]:

$$L_{mr} = 2s[(1 - \lambda_1 \lambda_2)(\delta_{mr} - N_m N_r) + i(\lambda_2 - \lambda_1) \varepsilon_{mrs} N_s + \eta_{1m} \eta_{2r} + \eta_{1r} \eta_{2m} - (\bar{\eta}_1 \bar{\eta}_2)(\delta_{mr} - N_m N_r)], \quad (5)$$

where λ_1 and λ_2 ($\bar{\eta}_1$ and $\bar{\eta}_2$) are the helicities (transverse components of the spin vectors) of the electron and the positron, \bar{N} is a unit vector directed along the momentum of the electron.

As for the fermionic tensor H_{mr} , we note that in the general case it is cumbersome and is therefore not given here. However, at high energies of the colliding particles ($\sqrt{s} \geq 1$ TeV), the ratio $\frac{m_f^2}{s}$ can be neglected in comparison with unity (for example, for the heaviest t -quark with a mass of 173.1 GeV, this ratio for $\sqrt{s} = 1$ TeV is $(\frac{173.1}{10^3})^2 = 0.03 \ll 1$). Then, neglecting the terms proportional to $\frac{m_f^2}{s}$ and $\frac{M_{H_{SM}}^2}{s}$, we have a simple expression for the fermionic tensor (the fermions are longitudinally polarized):

$$H_{mr} = \frac{x_H^2}{2x_{12}} [(1 + h_1 h_2)(\delta_{mr} - n_m n_r) - i(h_1 + h_2) \varepsilon_{mrs} n_s], \quad (6)$$

where $x_{12} = (1-x_1)(1-x_2)$, $x_1 = \frac{2E_1}{\sqrt{s}}$, $x_2 = \frac{2E_2}{\sqrt{s}}$ and $x_H = \frac{2E_H}{\sqrt{s}}$ are the scaling energies of the fermion, antifermion and Higgs boson, respectively, h_1 and h_2 are the helicities of the fermion and antifermion, \vec{n} is the unit vector along the Higgs momentum of the boson.

The product of the lepton and fermion tensors can be represented in the form:

$$L_{mr} \cdot H_{mr} = \frac{1}{2}(L_{11} + L_{22}) \cdot \sigma_1 + (L_{22} - L_{11}) \cdot \sigma_2 + L_{33} \cdot \sigma_3 + (L_{13} + L_{31}) \cdot \sigma_4 - (L_{23} + L_{32}) \cdot \sigma_5 - (L_{12} + L_{21}) \cdot \sigma_6 - \frac{i}{2}(L_{12} - L_{21}) \cdot \sigma_7 - i(L_{23} - L_{32}) \cdot \sigma_8 - i(L_{31} - L_{13}) \cdot \sigma_9, \quad (7)$$

where the so-called correlation functions are introduced σ_a ($a = 1 \div 9$), by means of relations:

$$\begin{aligned} \sigma_1 &= H_{11} + H_{22}, & \sigma_2 &= \frac{1}{2}(H_{22} - H_{11}), & \sigma_3 &= H_{33}, \\ \sigma_4 &= -\frac{1}{2}(H_{13} + H_{31}), & \sigma_5 &= -\frac{1}{2}(H_{23} + H_{32}), & \sigma_6 &= -\frac{1}{2}(H_{12} + H_{21}), \\ \sigma_7 &= i(H_{12} - H_{21}), & \sigma_8 &= \frac{i}{2}(H_{23} - H_{32}), & \sigma_9 &= \frac{i}{2}(H_{31} - H_{13}). \end{aligned} \quad (8)$$

We use the coordinate system in which the OXZ plane coincides with the plane of particle production $\vec{q}_1 + \vec{q}_2 + \vec{k} = 0$ and introduce the angles θ , χ and φ , where θ is the polar angle between the Z axis and the direction of the electron beam, χ – the azimuth angle between the production plane and the plane determined by the Z axis and the beam e^- , φ is the azimuth angle between the production planes and transverse polarization of the electron. In this system, the components of the vectors \vec{N} , $\vec{\eta}_1$ and $\vec{\eta}_2$ is determined by expressions

$$\begin{aligned} \vec{N} &= (\sin \theta \cdot \cos \chi, \sin \theta \cdot \sin \chi, \cos \theta), \\ \vec{\eta}_1 &= -\vec{\eta}_2 = (-\sin \theta \sin \chi \cos \varphi - \cos \chi \sin \varphi, -\cos \theta \sin \theta \cos \varphi - \cos \chi \sin \varphi, \sin \theta \cos \varphi). \end{aligned} \quad (9)$$

Then for the product of tensors $L_{mr} \cdot H_{mr}$ we have:

$$\begin{aligned} L_{mr} \cdot H_{mr} &= 2s(1 + h_1 h_2) \left\{ \frac{1}{2} [(1 - \lambda_1 \lambda_2)(1 + \cos^2 \theta) + \eta_1 \eta_2 \sin^2 \theta \cos 2\varphi] \sigma_1 + \right. \\ &+ [(1 - \lambda_1 \lambda_2) \sin^2 \theta \cos 2\chi - \eta_1 \eta_2 ((1 + \cos^2 \theta) \cos 2\chi \cos 2\varphi - 2 \sin \theta \sin \chi \sin 2\varphi)] \sigma_2 + \\ &+ [(1 - \lambda_1 \lambda_2) \sin^2 \theta - \eta_1 \eta_2 \sin^2 \theta \cos 2\varphi] \sigma_3 + [(1 - \lambda_1 \lambda_2) \sin^2 \theta \cos 2\chi + \eta_1 \eta_2 ((1 + \cos^2 \theta) \times \\ &\quad \times \sin 2\chi \cos 2\varphi + 2 \cos \theta \cos 2\chi \sin 2\varphi)] \sigma_4 + [(1 - \lambda_1 \lambda_2) \sin 2\theta \sin \chi - \\ &\quad - \eta_1 \eta_2 (\sin 2\theta \sin \chi \cos 2\varphi + 2 \sin \theta \cos \chi \sin 2\varphi)] \sigma_5 + \\ &\left. + [-(1 - \lambda_1 \lambda_2) \sin 2\theta \cos \chi - \eta_1 \eta_2 (\sin 2\theta \cos \chi \cos 2\varphi - 2 \sin \theta \sin \chi \sin 2\varphi)] \sigma_6 \right\} - \\ &- 2s(h_1 + h_2)(\lambda_1 - \lambda_2) [\cos \theta \cdot \sigma_7 + 2 \sin \theta (\cos \chi \cdot \sigma_8 + \sin \chi \cdot \sigma_9)]. \end{aligned} \quad (10)$$

2. Differential cross section of the reaction $e^- e^+ \rightarrow H_{SM} f \bar{f}$

Based on the general rules for the differential cross section of the process $e^- + e^+ \rightarrow H_{SM} + f + \bar{f}$, the following expression is obtained

$$\frac{d^5 \sigma}{d\chi d\varphi d(\cos \theta) dx_1 dx_2} = \frac{\alpha_{KED}^2 Q_f^2 N_C}{256 \pi^3 s} g_{H_{SM}ff}^2 \{ (1 + h_1 h_2) [(1 - \lambda_1 \lambda_2) \sigma_A +$$

$$+ \eta_1 \eta_2 (\cos 2\varphi \cdot \sigma_B - \sin 2\varphi \cdot \sigma_C)] + (\lambda_1 - \lambda_2)(h_1 + h_2)\sigma_D\}. \quad (11)$$

Here

$$\begin{aligned} \sigma_A &= \frac{1}{2}(1 + \cos^2 \theta)\sigma_1 + \sin^2 \theta(\cos 2\chi \cdot \sigma_2 + \sigma_3 + \sin 2\chi \cdot \sigma_4) + \sin 2\theta(\sin \chi \cdot \sigma_5 + \cos \chi \cdot \sigma_6), \\ \sigma_B &= \sin^2 \theta \left(\frac{1}{2}\sigma_1 - \sigma_3 \right) + (1 + \cos^2 \theta)(\cos 2\chi \cdot \sigma_2 + \sin 2\chi \cdot \sigma_4) - \sin 2\theta(\sin \chi \cdot \sigma_5 - \cos \chi \cdot \sigma_6), \quad (12) \\ \sigma_C &= 2 \cos \theta(\sin 2\chi \cdot \sigma_2 - \cos 2\chi \cdot \sigma_4) + 2 \sin \theta(\cos \chi \cdot \sigma_5 - \sin \chi \cdot \sigma_6), \\ \sigma_D &= \cos \theta \cdot \sigma_7 + 2 \sin \theta(\cos \chi \cdot \sigma_8 + \sin \chi \cdot \sigma_9), \end{aligned}$$

where N_C is the color factor (in the case of the production of a lepton pair $N_C = 1$, and in the case of the production of quarks $N_C = 3$).

The correlation functions σ_a ($a = 1 \div 9$) in (12) depend on the scaling energies x_1 and x_2 ($x_H = 2 - x_1 - x_2$) and they are easily determined on the basis of the fermionic tensor (6):

$$\begin{aligned} \sigma_1 &= \frac{x_H^2}{2x_{12}}(2 - n_x^2), & \sigma_2 &= \frac{x_H^2}{4x_{12}}n_x^2, & \sigma_3 &= \frac{x_H^2}{2x_{12}}(1 - n_z^2), \\ \sigma_4 &= \frac{x_H^2}{2x_{12}} \cdot n_x n_z, & \sigma_5 &= \sigma_6 = \sigma_9 = 0, & \sigma_7 &= \frac{x_H^2}{x_{12}} \cdot n_z, \\ \sigma_8 &= \frac{x_H^2}{2x_{12}} \cdot n_x, \end{aligned} \quad (13)$$

As can be seen, because of the orthogonality of the Y axis to the particle production plane, the correlation functions σ_5 , σ_6 and σ_9 vanish. Under the condition $\frac{M_H^2}{s} \ll 1$ and $\frac{m_f^2}{s} \ll 1$ the distribution of particles in the Dalitz diagram is determined by the laws of conservation of energy and momentum:

$$x_1 + x_2 + x_H = 2, \quad x_1 \vec{n}_1 + x_2 \vec{n}_2 + x_H \vec{n} = 0.$$

The boundaries of the allowed domain are determined by the equations $x_k = |x_i \pm x_j|$ ($i \neq j \neq k$). Direct $x_1 = x_2$, $x_1 = x_H$ and $x_2 = x_H$ divide the Dalitz diagram into six different regions. In the region ($i; j$) the scaling energies of the particles x_i and x_j satisfy the conditions

$$x_i \geq x_j \geq x_k \quad (i \neq j \neq k).$$

We can direct the axis Z along the most energetic particle and select the axis X so that the x -projection of the momentum of the second more energetic particle becomes positive. Then the following areas of the Dalitz diagram are obtained.

Ia (3; 1). The axis Z is directed along the momentum of a more energetic Higgs boson, and the momentum of the second energetic fermion has a positive x -projection (see Fig. 2a)

$$\vec{n} = (0, 0, 1), \quad \vec{n}_1 = (s_{31}, 0, c_{31}), \quad \vec{n}_2 = (-s_{32}, 0, c_{32}).$$

Similarly we have the reduced regions:

$$\mathbf{Ib(3; 2):} \quad \vec{n} = (0, 0, 1), \quad \vec{n}_1 = (-s_{31}, 0, c_{31}), \quad \vec{n}_2 = (s_{32}, 0, c_{32}).$$

$$\mathbf{IIa(1; 3):} \quad \vec{n}_1 = (0, 0, 1), \quad \vec{n}_2 = (-s_{12}, 0, c_{12}), \quad \vec{n} = (s_{13}, 0, c_{13});$$

$$\mathbf{IIb(1; 2):} \quad \vec{n}_1 = (0, 0, 1), \quad \vec{n}_2 = (s_{12}, 0, c_{12}), \quad \vec{n} = (-s_{13}, 0, c_{13});$$

$$\mathbf{IIIa(2; 3):} \quad \vec{n}_2 = (0, 0, 1), \quad \vec{n}_1 = (-s_{21}, 0, c_{21}), \quad \vec{n} = (s_{23}, 0, c_{23});$$

$$\mathbf{IIIb(2; 1):} \quad \vec{n}_2 = (0, 0, 1), \quad \vec{n}_1 = (s_{21}, 0, c_{21}), \quad \vec{n} = (-s_{23}, 0, c_{23}).$$

Here we have introduced the notation $s_{ij} = \sin \theta_{ij}$ and $c_{ij} = \cos \theta_{ij}$, where θ_{ij} – the angle between the directions of the particle momenta i and j . These angles depend on the scaling energies of the particles

$$\sin \theta_{ij} = \frac{2\sqrt{(1-x_1)(1-x_2)(1-x_H)}}{x_i x_j}, \quad \cos \theta_{ij} = 1 - \frac{2(x_i + x_j - 1)}{x_i x_j}. \quad (14)$$

Using these relations, we can easily determine the correlation functions in each region of the Dalitz diagram. Here we give the correlation functions in the coordinate system Ia (Ib), where the momentum of the more energetic Higgs boson is directed along the axis Z , and the second energetic fermion (antifermion) in the production plane has a positive momentum projection $q_{1x} > 0$ ($q_{2x} > 0$):

$$\sigma_1 = \sigma_7 = \frac{x_H^2}{(1-x_1)(1-x_2)} = 2 + \frac{1-x_1}{1-x_2} + \frac{1-x_2}{1-x_1}, \quad \sigma_2 = \sigma_3 = \sigma_4 = \sigma_8 = 0. \quad (15)$$

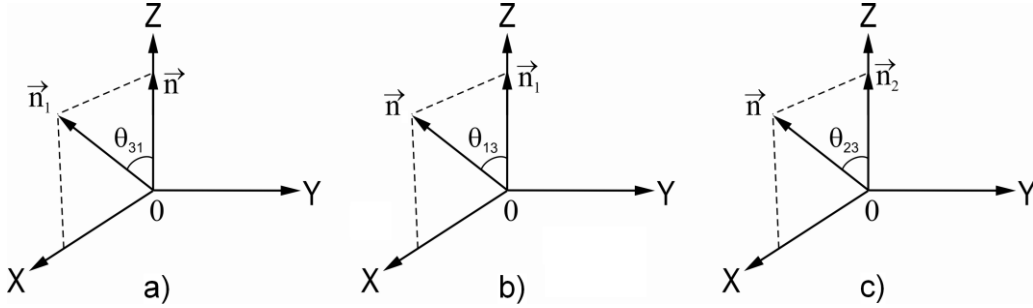


Fig. 2. Coordinate systems Ia, IIa and IIIa

Integrating the cross section (11) along the azimuthal angle φ , we obtain the particle distribution over the angles θ and χ in the case of longitudinally polarized e^-e^+ - and $f\bar{f}$ -pairs

$$\begin{aligned} \frac{d^4\sigma}{d\chi d(\cos\theta) dx_1 dx_2} &= \frac{\alpha_{KED}^2 Q_f^2 N_C}{256\pi^2 s} g_{H_{SM}ff}^2 (\sigma_1 + 2\sigma_3) \{ (1+h_1 h_2)(1-\lambda_1 \lambda_2) [1 + \alpha_1 \cos^2 \theta + \\ &+ \alpha_2 \sin^2 \theta \cos 2\chi + \alpha_4 \sin^2 \theta \sin 2\chi] + (h_1 + h_2)(\lambda_2 - \lambda_1) [\alpha_7 \cos \theta + \alpha_8 \sin \theta \cos \chi] \}, \end{aligned} \quad (16)$$

where the coefficients of the angular distributions of particles:

$$\alpha_1 = \frac{\sigma_1 - 2\sigma_3}{\sigma_1 + 2\sigma_3}, \quad \alpha_2 = \frac{2\sigma_2}{\sigma_1 + 2\sigma_3}, \quad \alpha_4 = \frac{2\sigma_4}{\sigma_1 + 2\sigma_3}, \quad \alpha_7 = \frac{2\sigma_7}{\sigma_1 + 2\sigma_3}, \quad \alpha_8 = \frac{4\sigma_8}{\sigma_1 + 2\sigma_3}. \quad (17)$$

It follows from the formula of the differential cross section (16) that the electron and the positron must have opposite helicities $\lambda_1 = -\lambda_2 = \pm 1$ (the electron is left, and the positron is right – $e_L^- e_R^+$, or the electron is right, and the positron is left – $e_R^- e_L^+$), while the helicities of the fermion and antifermion must be the same – $h_1 = h_2 = \pm 1$ (fermion and antifermion right – $f_R \bar{f}_R$ or left – $f_L \bar{f}_L$). Thus, four spiral sections correspond to the process $e^- + e^+ \rightarrow H_{SM} + f + \bar{f}$:

- 1) electron, fermion and antifermion are left polarized, and positron is right:

$$\begin{aligned} \frac{d^4\sigma(e_L^- e_R^+ \rightarrow H_{SM} f_L \bar{f}_L)}{d\chi d(\cos\theta) dx_1 dx_2} &= \frac{\alpha_{KED}^2 Q_f^2 N_C}{64\pi^2 s} g_{H_{SM}ff}^2 (\sigma_1 + 2\sigma_3) [1 + \alpha_1 \cos^2 \theta + \\ &+ \alpha_2 \sin^2 \theta \cos 2\chi + \alpha_4 \sin^2 \theta \sin 2\chi - \alpha_7 \cos \theta - \alpha_8 \sin \theta \cos \chi]; \end{aligned}$$

2) the electron, fermion and antifermion are right polarized, and the positron is left:

$$\frac{d^4\sigma(e_R^-e_L^+ \rightarrow H_{SM}f_R\bar{f}_R)}{d\chi d(\cos\theta)dx_1dx_2} = \frac{\alpha_{KED}^2 Q_f^2 N_C}{64\pi^2 s} g_{H_{SM}ff}^2 (\sigma_1 + 2\sigma_3)[1 + \alpha_1 \cos^2 \theta + \alpha_2 \sin^2 \theta \cos 2\chi + \alpha_4 \sin^2 \theta \sin 2\chi - \alpha_7 \cos \theta - \alpha_8 \sin \theta \cos \chi];$$

3) the electron is polarized to the left, and the positron, fermion, and antifermion are right:

$$\frac{d^4\sigma(e_L^-e_R^+ \rightarrow H_{SM}f_R\bar{f}_R)}{d\chi d(\cos\theta)dx_1dx_2} = \frac{\alpha_{KED}^2 Q_f^2 N_C}{64\pi^2 s} g_{H_{SM}ff}^2 (\sigma_1 + 2\sigma_3)[1 + \alpha_1 \cos^2 \theta + \alpha_2 \sin^2 \theta \cos 2\chi + \alpha_4 \sin^2 \theta \sin 2\chi + \alpha_7 \cos \theta + \alpha_8 \sin \theta \cos \chi];$$

4) the electron is polarized right, and the positron, fermion and antifermion are left:

$$\frac{d^4\sigma(e_R^-e_L^+ \rightarrow H_{SM}f_L\bar{f}_L)}{d\chi d(\cos\theta)dx_1dx_2} = \frac{\alpha_{KED}^2 Q_f^2 N_C}{64\pi^2 s} g_{H_{SM}ff}^2 (\sigma_1 + 2\sigma_3)[1 + \alpha_1 \cos^2 \theta + \alpha_2 \sin^2 \theta \cos 2\chi + \alpha_4 \sin^2 \theta \sin 2\chi + \alpha_7 \cos \theta + \alpha_8 \sin \theta \cos \chi].$$

It is of interest to compare the cross sections of processes $e^- + e^+ \rightarrow q + \bar{q} + g$ and $e^- + e^+ \rightarrow q + \bar{q} + H_{SM}$ in the case of longitudinally polarized particles, where g – the gluon emitted by the quark and antiquark. Calculations show that in the process $e^- + e^+ \rightarrow q + \bar{q} + g$ the quark and antiquark must possess opposite helicities ($q_L\bar{q}_R$ or $q_R\bar{q}_L$) [16]. In the process $e^- + e^+ \rightarrow q + \bar{q} + H_{SM}$ considered here, the quark and antiquark should be polarized either left ($q_L\bar{q}_L$) or right ($q_R\bar{q}_R$)

We estimate the coefficients of the angular distributions α_i ($i=1, 2, 4, 7, 8$) in the coordinate system IIIa, where the momentum of the antifermion is oriented along the Z axis, and the momentum of Higgs boson in the production plane has a positive x-projection (Fig. 2c). Using the expressions for the correlation functions given in the Appendix, for these coefficients we have the expressions:

$$\alpha_1 = \frac{3c_{23}^2 - 1}{3 - c_{23}^2}, \quad \alpha_2 = \frac{s_{23}^2}{3 - c_{23}^2}, \quad \alpha_4 = -\frac{2s_{23}c_{23}}{3 - c_{23}^2}, \quad \alpha_7 = \frac{4c_{23}}{3 - c_{23}^2}, \quad \alpha_8 = -\frac{4s_{23}}{3 - c_{23}^2}.$$

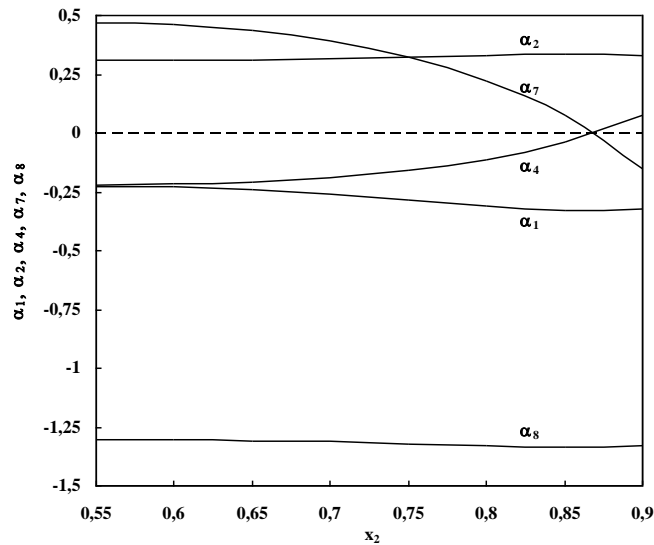


Fig.3. Dependence of the angular distribution coefficients on x_2 at $x_1 = 0,9$ in the reaction $e^-e^+ \rightarrow H_{SM}\tau^-\tau^+$.

Fig. 3 shows the dependence of the angular distribution coefficients on the scaling energy x_2 for a fixed $x_1 = 0,9$ in process $e^- + e^+ \rightarrow H_{SM} + \tau^- + \tau^+$. As can be seen, the coefficients α_1 and α_8 are negative and decrease x_2 slowly with increasing. The coefficient α_2 is positive and increases x_2 slowly with increasing. As for the coefficients α_4 and α_7 , we note that at the beginning of the spectrum the coefficient α_4 (α_7) is negative (positive) and with increasing x_2 it monotonically increases (decreases) and vanishes, and then becomes positive (negative).

Summing (averaging) the differential cross section (16) over the polarization states of the anti-fermion (positron) and integrating with respect to the angle χ , we have

$$\frac{d^3\sigma}{d(\cos\theta)dx_1dx_2} = \frac{\alpha_{KED}^2 Q_f^2 Nc}{128\pi s} g_{H_{SM}ff}^2 (\sigma_1 + 2\sigma_3) \times [1 + \alpha_1(x_1, x_2) \cos^2\theta - h_1 \lambda_1 \alpha_7(x_1, x_2) \cos\theta]. \quad (18)$$

It follows that if the electron is longitudinally polarized, then in the process $e^- + e^+ \rightarrow H_{SM} + f + \bar{f}$ the fermion can acquire longitudinal polarization. The degree of longitudinal polarization of the fermion is determined in the standard manner

$$P_f(x_1, x_2, \cos\theta) = -\lambda_1 \cdot \frac{\alpha_7(x_1, x_2) \cos\theta}{1 + \alpha_1(x_1, x_2) \cos^2\theta}. \quad (19)$$

The degree of longitudinal polarization (19) can be conveniently investigated in the process $e^- + e^+ \rightarrow H_{SM} + \tau^- + \tau^+$, since by investigating the decay channels in $\tau^- \rightarrow \pi^- + \nu_\tau$, $\tau^- \rightarrow K^- + \nu_\tau$ experiments it is possible to determine the degree of longitudinal polarization of the τ^- -lepton.

Fig. 4 illustrates the angular dependence of the degree of longitudinal polarization of a τ^- -lepton for $\lambda_1 = -1$ a fixed $x_1 = 0,9$, $x_2 = 0,6$ and $x_1 = 0,9$, $x_2 = 0,8$. As can be seen, with increasing angle θ , the degree of longitudinal polarization decreases and reaches a minimum at the end of the angular spectrum. The growth of the scaling energy x_2 leads to a decrease in the degree of longitudinal polarization of the τ^- -lepton.

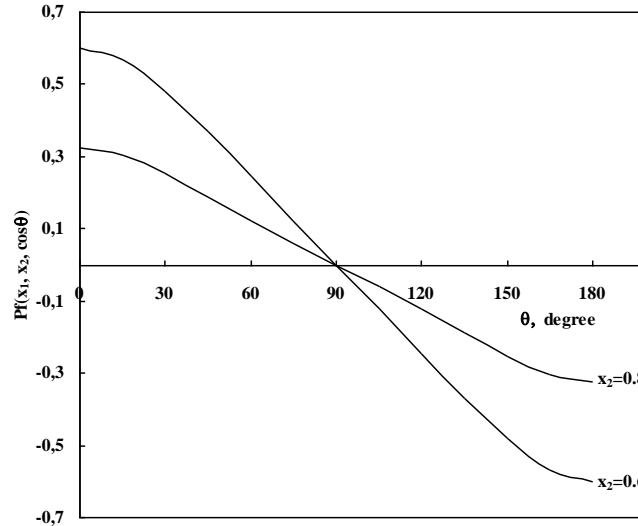


Fig. 4. Angular dependence of the degree of longitudinal polarization of τ^- -lepton

Fig. 5 shows the dependence of the degree of longitudinal polarization of τ^- -lepton on the change x_2 for a fixed energy $x_1 = 0,9$ and for different angles θ of emission of particles. When the degree $0 \leq \theta < 90^\circ$ of longitudinal polarization it is positive, and for $90^\circ < \theta \leq 180^\circ$ it is negative.

Now consider the particle distribution over the angles θ and φ . To do this, we integrate the cross section (11) along the azimuthal angle χ of the (e^-e^+ -pair is polarized transversely):

$$\frac{d^4\sigma}{d\varphi d(\cos\theta)dx_1dx_2} = \frac{\alpha_{KED}^2 Q_f^2 N_C}{128\pi^2 s} g_{H_{SM}}^2 (\sigma_1 + 2\sigma_3)(1 + \alpha_1 \cos^2 \theta) \times [1 + A_{\perp}(x_1, x_2, \cos\theta)\eta_1\eta_2 \cos 2\varphi]. \quad (20)$$

Here $A_{\perp}(x_1, x_2, \cos\theta)$ is the transverse spin asymmetry due to the transverse polarizations of the e^-e^+ -pair and determined by the relation

$$A_{\perp}(x_1, x_2, \cos\theta) = \frac{\alpha_1(x_1, x_2) \sin^2 \theta}{1 + \alpha_1(x_1, x_2) \cos^2 \theta}. \quad (21)$$

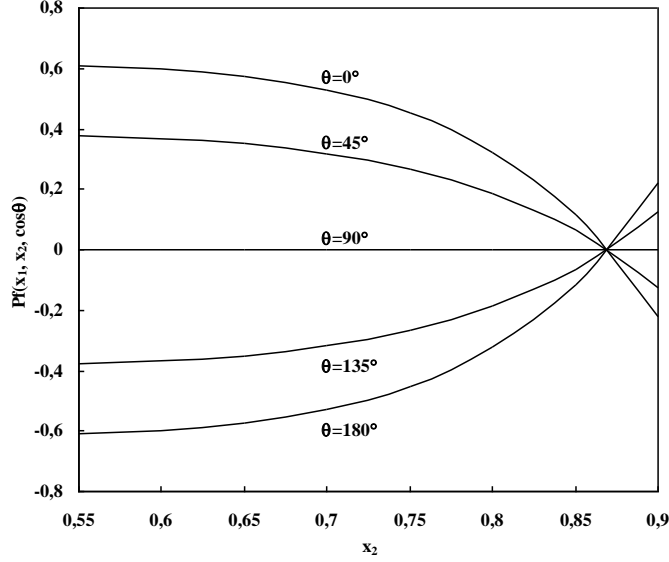


Fig. 5. The dependence of the degree of longitudinal polarization of a τ^- -lepton on the change x_2 at a fixed energy $x_1 = 0,9$ and different angles θ of emission of particles.

Fig. 6 illustrates the angular dependence of the transverse spin asymmetry in the process $e^- + e^+ \rightarrow H_{SM} + \tau^- + \tau^+$ for a fixed $x_1 = 0,95$, $x_2 = 0,55$ and $x_2 = 0,65$. As the angle θ increases, the degree of transverse spin asymmetry increases and reaches a maximum at $\theta = 90^\circ$, and a further increase of the angle leads to a decrease in the asymmetry. With increasing scaling energy x_2 , the transverse spin asymmetry decreases.

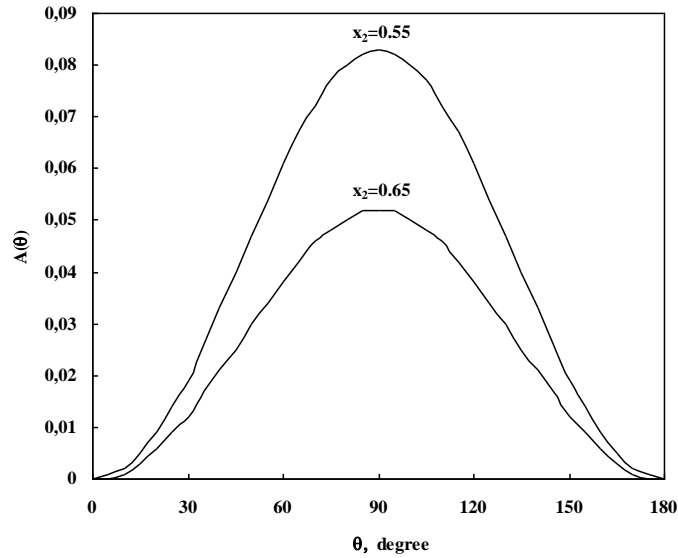


Fig. 6. Angular dependence of the transverse spin asymmetry in the process $e^-e^+ \rightarrow H_{SM}\tau^-\tau^+$.

Integrating the cross section (20) over the angles θ and φ , we obtain the energy spectrum of the particles, which

coincides with the result of [17]

$$\frac{d^2\sigma}{dx_1 dx_2} = \frac{\alpha_{KED}^2 Q_f^2 N_C}{12\pi s} g_{H_{SM} ff}^2 \cdot \left(2 + \frac{1-x_1}{1-x_2} + \frac{1-x_2}{1-x_1} \right). \quad (22)$$

Fig. shows the dependence of the differential cross section (22) on the variable x_2 for fixed $x_1 = 0,9$ and $0,95$. As the variable x_2 increases, the differential cross section decreases monotonically, and the growth of the τ^- -lepton energy x_1 leads to an increase in the cross section.

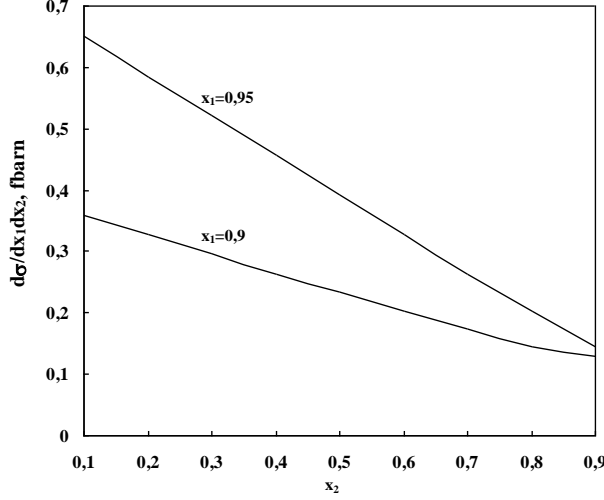


Fig. 7. The dependence of the differential cross section of the process $e^-e^+ \rightarrow H_{SM}\tau^-\tau^+$ from a variable x_2 for a fixed $x_1 = 0,9$ and $0,95$

We introduce new variables $T = T_1 = \max(x_1, x_2, x_H)$, T_2 and T_3 so that the inequalities $T = T_1 \geq T_2 \geq T_3 = 2 - T - T_2$ are satisfied. We select the axis Z along the momentum of the most energetic particle and carry out integration over the variable T_2 for a fixed T one. As a result, we find the cross section $\frac{d\sigma}{dT}$ of the process $e^- + e^+ \rightarrow H_{SM} + f + \bar{f}$ as a function T . For $x_H = T$ and $x_1 = T_2$ and (or $x_2 = T_2$) the cross section is:

$$\frac{d\sigma}{dT} = \frac{\alpha_{KED}^2 Q_f^2 N_C}{12\pi s} g_{H_{SM} ff}^2 \cdot T \ln\left(\frac{1-T}{T}\right). \quad (23)$$

For $x_1 = T$ and $x_H = T_2$ (or for $x_2 = T$ and $x_H = T_2$) we have a section:

$$\frac{d\sigma}{dT} = \frac{\alpha_{KED}^2 Q_f^2 N_C}{12\pi s} g_{H_{SM} ff}^2 \cdot \left[\frac{(3T-2)(6-5T)}{2(1-T)} - (1-T) \ln\left(\frac{2T-1}{1-T}\right) \right]. \quad (24)$$

If, however, $x_1 = T$ and $x_2 = T_2$ (or if $x_2 = T$ and $x_1 = T_2$), then the cross section

$$\frac{d\sigma}{dT} = \frac{\alpha_{KED}^2 Q_f^2 N_C}{12\pi s} g_{H_{SM} ff}^2 \cdot \left[\frac{(3T-2)(2-T)}{2(1-T)} + (1-T) \ln\left(\frac{2T-1}{T}\right) \right]. \quad (25)$$

Adding the expressions (23)-(25), we obtain a section characterizing the distribution of the most energetic particle with respect to the variable T :

$$\frac{d\sigma}{dT} = \frac{\alpha_{KED}^2 Q_f^2 N_C}{12\pi s} g_{H_{SM} ff}^2 \cdot \left[\frac{(3T-2)(4-3T)}{1-T} + \ln\left(\frac{2T-1}{T}\right) \right]. \quad (26)$$

Fig. 8 shows the dependence of the reaction $e^- + e^+ \rightarrow H_{SM} + \tau^- + \tau^+$ cross section on the variable T for $\sqrt{s} = 1$ TeV and $m_\tau = 1,778$ GeV. An increase in the variable T from $0,725$ to $0,9$ leads to a monotonic increase in the cross section of the reaction from $0,012$ fbarn to $0,448$ fbarn.

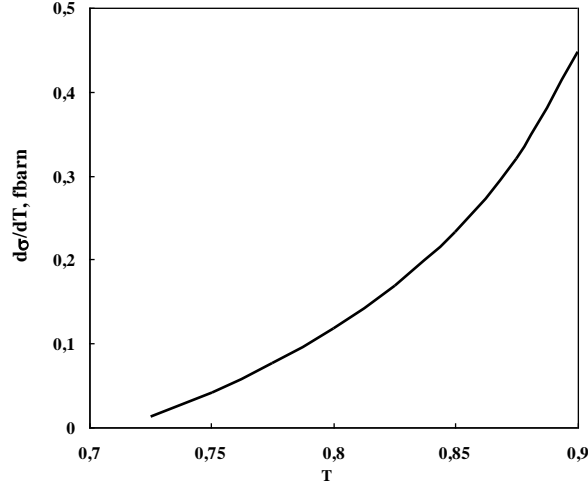


Fig. 8. The dependence of the cross section of the process $e^-e^+ \rightarrow H_{SM}\tau^-\tau^+$ on the variable T .

4. The production of the Higgs bosons of the MSSM and the fermion pair

Along with SM, the Minimal Supersymmetric Standard Model (MSSM) [7, 18] is widely discussed in the literature, where two doublets of a complex scalar field with hypercharges -1 and +1 are introduced:

$$\varphi_1 = \begin{pmatrix} H_1^0 \\ H_1^- \end{pmatrix}, \quad \varphi_2 = \begin{pmatrix} H_2^+ \\ H_2^0 \end{pmatrix}.$$

After the spontaneous breaking of the MSSM, five Higgs particles appear: CP-even h - and H -bosons, CP-odd A -boson and charged H^+ - and H^- -bosons. In high-energy electron-positron collisions, in addition to the process $e^- + e^+ \rightarrow H_{SM} + f + \bar{f}$, there can also occur reactions of the production of Higgs bosons MSSM and the fermion pair: $e^- + e^+ \rightarrow H + f + \bar{f}$, $e^- + e^+ \rightarrow h + f + \bar{f}$ and $e^- + e^+ \rightarrow A + f + \bar{f}$. According to the MSSM, the interaction constants of these bosons with the fermion pair are determined by the expressions [18]:

$$g_{Hff} = \frac{m_f}{\eta} \cdot \frac{\sin \alpha}{\sin \beta}, \quad g_{hff} = \frac{m_f}{\eta} \cdot \frac{\cos \alpha}{\sin \beta}, \quad g_{Aff} = \frac{m_f}{\eta} \cdot \text{tg} \beta,$$

where α and β are the MSSM parameters. Consequently, the differential cross sections of the processes $e^- + e^+ \rightarrow H + f + \bar{f}$ and $e^- + e^+ \rightarrow h + f + \bar{f}$ will differ from the reaction $e^- + e^+ \rightarrow H_{SM} + f + \bar{f}$ cross section by the presence of an additional factor $\frac{\sin \alpha}{\sin \beta}$ and $\frac{\cos \alpha}{\sin \beta}$. As for the process $e^- + e^+ \rightarrow A + f + \bar{f}$, we note that, because of the pseudoscalarity of the A -boson, the expression for the fermion current (3) is replaced by the current:

$$J_\mu = \bar{u}_f(q_1) \left[\gamma_5 \frac{\hat{q}_1 + \hat{k} + m_f}{(q_1 + k)^2 - m_f^2} \gamma_\mu - \gamma_\mu \frac{\hat{q}_2 + \hat{k} - m_f}{(q_2 + k)^2 - m_f^2} \gamma_5 \right] v_f(q_2).$$

Note that this current also leads to the results obtained earlier for the reaction $e^- + e^+ \rightarrow H_{SM} + f + \bar{f}$. Here, too, it is necessary to replace the interaction constant $g_{H_{SM}ff}$ by the constant g_{Aff} .

CONCLUSION

We discussed the processes production of a Higgs boson H_{SM} (boson MSSM H, h, A) and a heavy fermion e^-e^+ -pair in annihilation of an arbitrarily polarized pair: $e^- + e^+ \rightarrow H_{SM} + f + \bar{f}$, $e^- + e^+ \rightarrow H + f + \bar{f}$, $e^- + e^+ \rightarrow h + f + \bar{f}$, $e^- + e^+ \rightarrow A + f + \bar{f}$. Analytical expressions are obtained for differential cross sections, angular and spin correlations. The features of the behavior of the cross sections, angular and spin correlations are investigated as a function of the energies and emission angles of the particles. The results are illustrated by graphs.

APPENDIX

Here we give the expressions for the correlation functions in coordinate systems IIa,b and IIIa, b

1) In systems IIa and IIb:

$$\begin{aligned}\sigma_1 &= \frac{x_H^2}{2x_{12}} (2 - s_{13}^2), & \sigma_2 &= \frac{x_H^2}{4x_{12}} \cdot s_{13}^2, \\ \sigma_3 &= \frac{x_H^2}{2x_{12}} (1 - c_{13}^2), & \sigma_4 &= \pm \frac{x_H^2}{2x_{12}} \cdot s_{13}c_{13}, \\ \sigma_7 &= \frac{x_H^2}{4x_{12}} \cdot c_{13}, & \sigma_8 &= \pm \frac{x_H^2}{2x_{12}} \cdot s_{13};\end{aligned}$$

2) In systems IIIa and IIIb:

$$\begin{aligned}\sigma_1 &= \frac{x_H^2}{2x_{12}} \cdot (2 - s_{23}^2), & \sigma_2 &= \frac{x_H^2}{2x_{12}} \cdot \frac{1}{2} s_{23}^2, \\ \sigma_3 &= \frac{x_H^2}{2x_{12}} \cdot (1 - c_{23}^2), & \sigma_4 &= \pm \frac{x_H^2}{2x_{12}} \cdot s_{23}c_{23}, \\ \sigma_7 &= \frac{x_H^2}{2x_{12}} \cdot 2c_{23}, & \sigma_8 &= \pm \frac{x_H^2}{2x_{12}} \cdot c_{23}.\end{aligned}$$

The upper sign corresponds to systems IIa and IIIa, and the lower sign corresponds to IIb and IIIb.

-
- [1] S.K. *Abdullayev*. Standart model, lepton və kvarkların xassələri. Bakı, «Zəka print», 2017, 274s.
- [2] A. *Djouadi*. The Anatomy of Electro-Weak Symmetry Breaking. Tome I: The Higgs boson in the Standard Model. arXiv: hep-ph/0503172v2, 2005; DOI: 10.1016/j.physrep.2007.10.004
- [3] ATLAS Collaboration. Observation of a new particle in the search for the Standard Model Higgs boson with the ATLAS detector at the LHC // Phys. Letters, 2012, B 716, p. 1-29
- [4] CMS Collaboration. Observation of a new boson at mass of 125 GeV with the CMS experiment at the LHC // Phys. Letters, B 716, p. 30-61.
- [5] P.W. *Higgs*. Broken Symmetries and the masses of gauge bosons // Phys. Rev. Lett., 1964, V. 13, p.508.
- [6] C.A. *Lester*. Search for the Higgs boson produced in association with top quarks in multilepton final states at ATLAS, University of Pensilvania, ScholarlyCommons. <http://repository.yenn.edn/edissertations>, 2015.
- [7] R.R. *Barman et al.* Current status of MSSM Higgs sector with LHC 13 TeV data // arXiv: 1608.02573v3 [hep-ph]. 2017 23 may.
- [8] S.K. *Abdullayev*, M.Sh. *Gojayev*, F.A. *Saddigh*. Decay Channels of the Standard Higgs Boson // Moscow University Physics Bulletin, 2017, Vol.72, №4, pp.329-339; published in Vestnik Moskovskoqo Universiteta, Seriya 3: Physics, Astronomy, 2017, №4, s.3-11.
- [9] S.K. *Abdullayev*, M.Sh. *Gojayev*, N.E. *Nesibova*. Production of scalar boson and neutrino pair in longitudinally polarized electron-positron colliding beams // Azerbaijan Journal of Physics: Fizika, 2017, XXIII, N. 3, p. 45-52.
- [10] S.K. *Abdullayev*, M.Sh. *Gojayev*, N.E. *Nesibova*. Rojdeniye skalyarnoqo bozona i fermionnoy pari na proizvolno polyarizovannix e⁻e⁺-puchkax // Izvestiya VUZov, Fizika, 2018, t. , s. (in Russian).
- [11] S.K. *Abdullayev*, M.Sh. *Gojayev*. The Higgs bosons production in arbitrary polarized electron-positron colliding beams // UZFF Moskovskoqo Universiteta, 2018. N. 1. s.1810101-1 (in Russian).
- [12] S.K. *Abdullayev*, M.Sh. *Gojayev*, N.E. *Nesibova*, G.A. *Soltanova*. The production of the higgs boson and t \bar{t} -pair in polarized e⁻e⁺-beams // Azerbaijan Journal of Physics: Fizika, 2018, XXIV, N. 1, p. 33-40.
- [13] V.D. *Shiltsev*. High-energy particle colliders: past 20 years, next 20 years, and beyond // Physics-Uspexhi, 2012, Vol. 55, N. 10, p.965-976.
- [14] K. *Peters*. Prospects for beyond Standard Model Higgs boson searches at future LHC runs and other machines // arXiv: 1701.05124v2 [hep-ex]. 2017
- [15] Gunion J.F. Muon Colliders: The Machine and The Physics. Preprint UCD-97-17, July 1997, University of California-Davis.
- [16] S.K. *Abdullayev*. Effects of the superstring Z' boson in the reactions e⁻e⁺ → qq \bar{g} and e⁻e⁺ → q \bar{q} g // Physics of Atomic Nuclei, 1997, V. 60, N. 11, p. 1901-1919.
- [17] K.J.F. *Gaemers*, G.J. *Gounaris*. Bremsstrahlung Production of Higgs boson in e⁻e⁺-collisions // Phys. Lett., 1978, V. 77B, N. 4-5, p. 379-382.
- [18] A. *Djouadi*. The Anatomy of Electro-Weak Symmetry Breaking. Tome II: The Higgs in Minimal Supersymmetric Model. arXiv: hep-ph/0503173v2, 2003;

Received: 18.09.2018